Nano Today 17 (2017) 14–22

Contents lists available at ScienceDirect

Nano Today

journal homepage: www.elsevier.com/locate/nanotoday

Rapid Communication

High-sensitivity molecular sensing using plasmonic nanocube chains in classical and quantum coupling regimes

Nasrin Hooshmand[a,b,1], Hamed Shams Mousavi[c,1], Sajanlal R. Panikkanvalappil[a], Ali Adibi[c], Mostafa A. El-Sayed[a,*]

[a] Laser Dynamics Laboratory, School of Chemistry and Biochemistry, Georgia Institute of Technology, Atlanta, GA 30332, United States
[b] Department of Chemistry, Marvdasht Branch, Islamic Azad University, Marvdasht, Iran
[c] School of Electrical and Computer Engineering, Georgia Institute of Technology, Atlanta, GR 30332, United States

ARTICLE INFO

Article history:
Received 11 July 2017
Received in revised form 7 September 2017
Accepted 30 October 2017
Available online 15 November 2017

Keywords:
DDA
FDTD
LSPR Coupling
Nanocubes
Orientation
Quantum corrected model
Classical coupling
Tunneling-induced charge transfer plasmons
Sensitivity
Assembly
Plasmonic nanoparticles
Sub-nanometer
Sensing

ABSTRACT

One-dimensional plasmonic nanoparticle arrays have intriguing optical properties that can be utilized in a number of applications, including molecular sensing. In this paper, firstly, we studied the plasmonic coupling behavior in chains of gold and silver plasmonic nanocubes of 21 nm edge length arranged in both face-to-face and edge-to-edge configurations at large separation distance (8.5 nm), where the classical electromagnetic coupling is dominant. Interestingly, an increase in the sensitivity factor was observed when increasing the number of nanocubes in the chain and by orienting them in edge-to-edge configuration, with a few exceptions. Additionally, linear chains of edge-to-edge and face-to-face assembled gold nanocube with sub-nanometer interparticle distances (0.2 nm), where the effect of tunneling-induced charge transfer plasmons (tCTPs) becomes significant, was studied using a quantum-corrected model. In comparison to the face-to-face orientation, the changes in optical properties were more prominent in the edge-to-edge configuration. Our results suggest that plasmonic coupling in linearly assembled nanoparticles becomes extremely important at sub-nanometer interparticle distances. It can significantly modify the optical properties of the nanocubes chains, especially spectral line shape and electric-field distribution, which might help designing more advanced sensing devices for chemical and bio-sensing applications.

Introduction

Gold and silver plasmonic nanoparticles possess unique optical properties due to their localized surface plasmon resonance (LSPR) and have promising applications in bio-imaging, labeling, optical energy transport, and chemical and biological sensing [1–13]. These resonant modes arise from the confinement of surface plasmons, which are the collective oscillation of the free electrons in the conduction band of metals [3,14–17] The LSPR wavelength (λ_{res}) can be tuned by changing the morphology (size and shape) of the nanoparticle or by changing the refractive index of the surrounding medium [4,18–26]. It is also known that when the nanoparticles are located in close proximity to one another, the coupling between these optical nanorasonators results in the hybridization of individual LSPR bands [27–29]. In our pervious works [30–34], we have shown that the near-field interaction between closely placed cubic Ag nanoparticles, as well as the far-field interaction in plasmonic lattices [35,36] is distance and orientation dependent.

In the present work, Ag and Au nanocubes (AgNCs and AuNCs) chains at classical coupling regime were first studied using discrete dipole approximation (DDA) method. Next, this classical study was complemented by analyzing AuNCs in quantum-coupling regime using a quantum-corrected finite-difference time-domain (FDTD) model, carried out in order to understand the role of plasmon tunneling as a new contribution component across nanoscale interfaces.

Using the DDA method, the intensity and spectral position of the plasmon bands and the corresponding field distribution around AgNCs and AuNCs chains in the edge-to-edge (EE) and face-to-face (FF) configurations were calculated in classical coupling regime.

* Corresponding author at: Laser Dynamics Laboratory, School of Chemistry and Biochemistry, Georgia Institute of Technology, Atlanta, GA 30332, United States.
E-mail address: melsayed@gatech.edu (M.A. El-Sayed).
[1] N. H. and H. M. contributed equally to this work.

https://doi.org/10.1016/j.nantod.2017.10.009
1748-0132/

Previously, the coupled LSPR modes of chains of noble metal nanoparticles, fabricated lithographically on a substrate, have been studied for low-loss energy transfer and low-loss sub-wavelength interconnection [37–39]. The potential of the closely-spaced plasmonic nanoparticle chains in molecular sensing based on the detection of the LSPR wavelength shift and surface enhanced Raman spectroscopy (SERS) has also been explored by several groups. It has been shown that well-engineered chains of plasmonic nanoparticles can provide a significant increase in sensitivity relative to conventional plasmonic sensors consisting of isolated or randomly placed nanoparticles [40–42]. Plasmonic nanoparticles exhibit high refractive index sensitivities, which is critical for developing powerful sensing devices [43–46]. The aptness of linear assemblies of plasmonic nanoparticles in sensing applications was further studied by calculating the sensitivity factor for the chains of Au and Ag NCs. Furthermore, we have investigated the optical properties of chains of Au and Ag NCs in EE and FF configurations and discussed its potential for sensing applications based on both LSPR resonance wavelength shift and SERS.

Numerical method

DDA is one of the most powerful theoretical techniques[47] for modeling the optical properties of plasmonic nanoparticles of arbitrary geometry. This method is used to calculate near field interaction between closely spaced Ag and Au nanocubes (edge length of 21 nm) assembled in EE and FF orientations on a glass substrate. The refractive index of surrounding medium (cap layer) is varied from 1.33 to 1.63 and the refractive index of AgNCs and AuNCs are assumed to be the same as that of the bulk metal [48]. In DDA, the target (here AgNCs or AuNCs on a substrate) is represented as cubic chains of several thousand points of acquired dipole moment in response to the local electric field located on a cubic lattice (with volume d^3). The response of each dipole to both the external field and neighboring dipoles are solved using Maxwell's equations. We have calculated the extinction spectra and field distribution around the surface of the AgNC and AuNC chains in both orientations (FF and EE), where the plasmonic field enhancement factor (in log scale of $|E|^2/|E_0|^2$) is located on the surface of a pair of cubes and calcu-

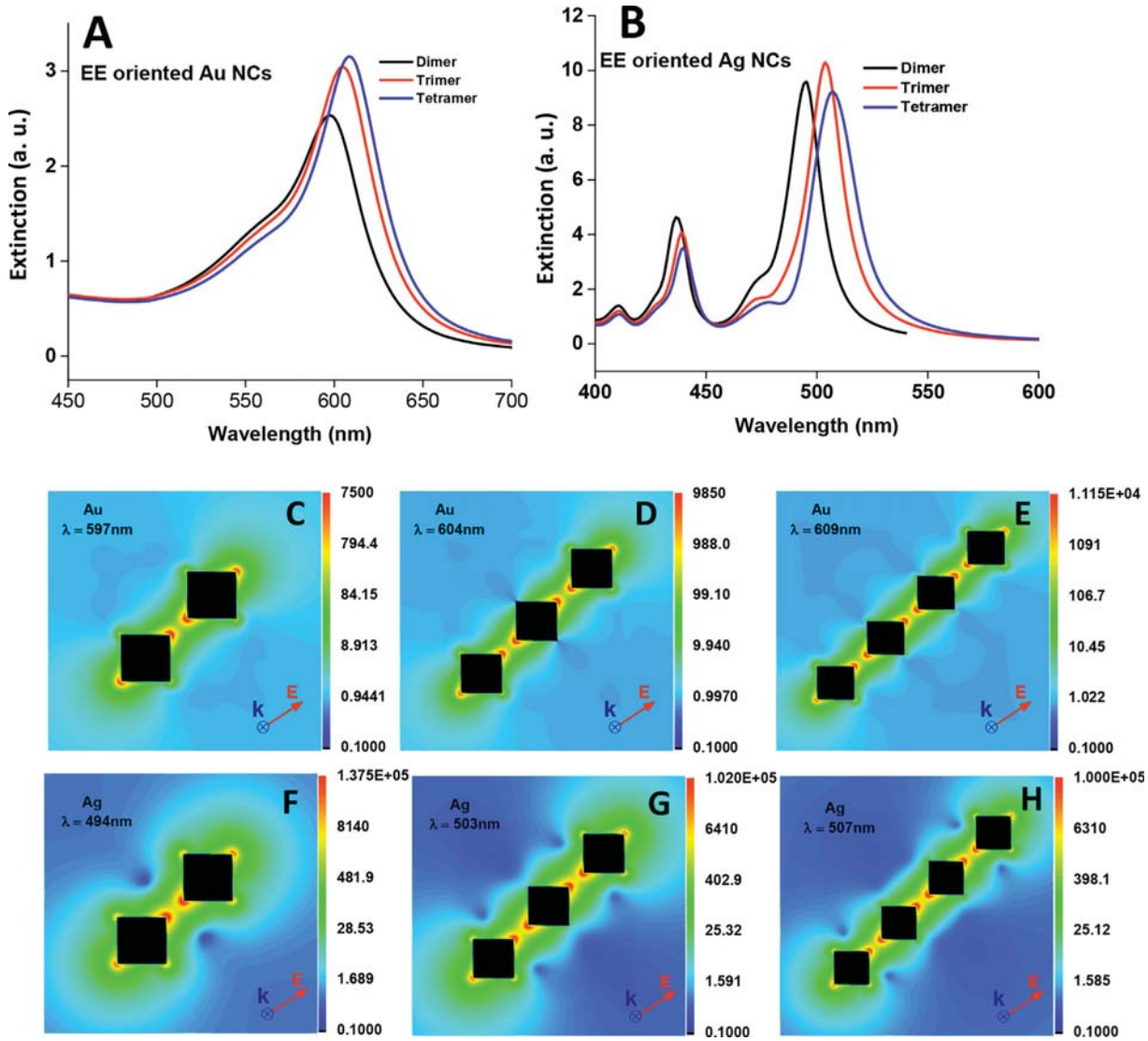

Fig. 1. DDA calculated extinction spectra and field distribution for EE oriented Ag and Au NC dimer, trimer, and tetramer with a separation distance of 8.5 nm in a surrounding medium of water on a glass substrate. As the number of cubes increases, a significant red shift in the extinction spectra of the both AuNCs and AgNCs was observed. In Au chains, the extinction cross-section of the chain is continuously increased as the number of cubes is increased (A, B). Whereas, in AgNCs we observe a decrease in extinction cross-section, when going from trimer to tetramer. Theoretical calculations of electromagnetic field distribution show that the maximum field enhancement around the Ag NCs is much higher than that of the Au NCs under similar conditions (C–H).

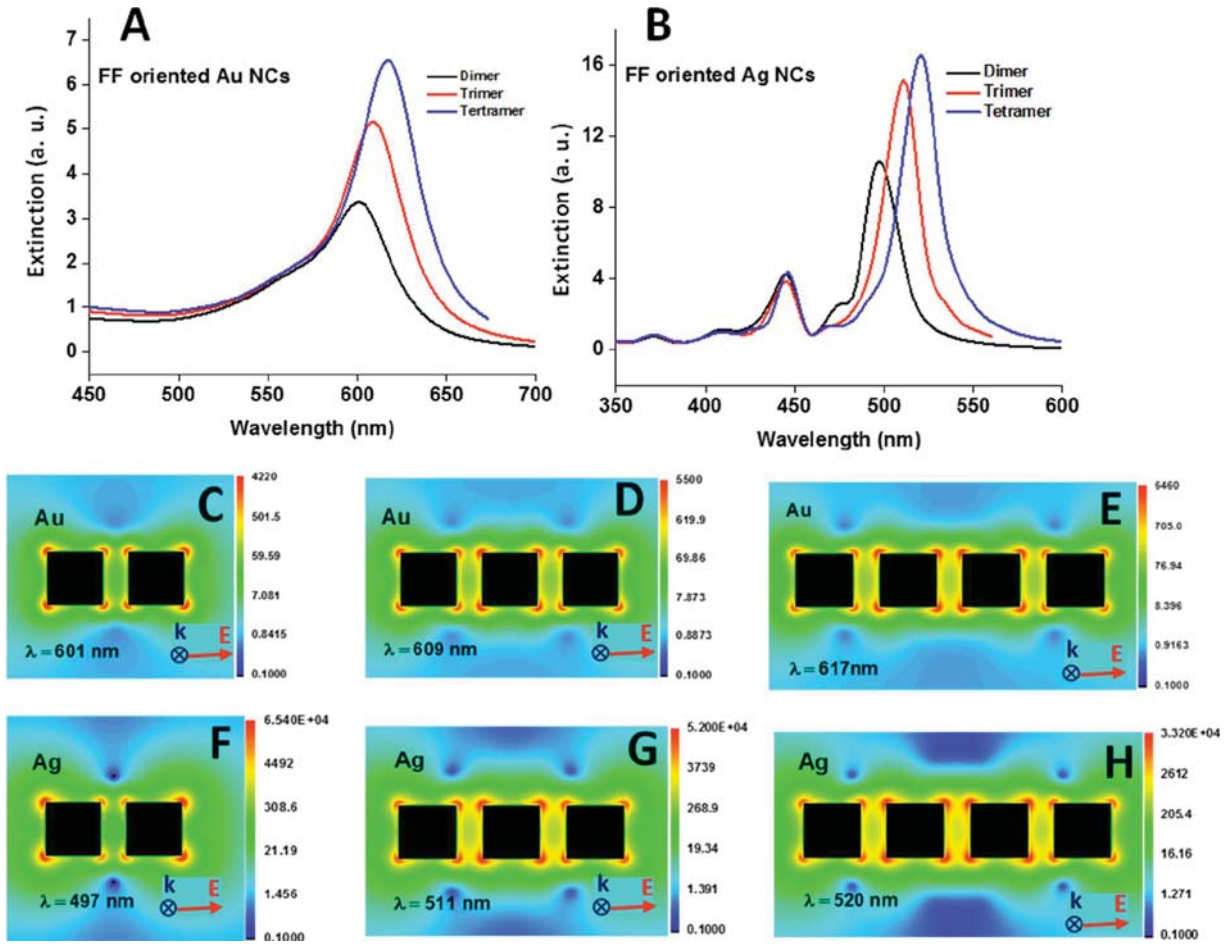

Fig. 2. DDA calculated extinction spectra and field distribution for the FF oriented Au and Ag NCs dimer, trimer, and tetramer with a separation distance of 8.5 nm in a surrounding medium of water on a glass substrate (A and B). As the number of cubes increases, a significant red shift in the extinction spectra of AgNCs is observed. Whereas, for the AuNCs, the intensity is continuously increased as the number of cubes increased. The maximum field enhancement around the, Ag nanocubes was more than ten times greater than that of the AuNCs under similar conditions (C–H).

lated with the DDA technique at different excitation wavelengths. We have included data for the FF oriented nanocubes along the dimer axis and for the EE oriented dimer along the diagonal of two cubes. Details of the DDA method have been described elsewhere [47,49,50].

Finite-difference time-domain (FDTD) [35] is another powerful analytical technique, widely used in plasmonics, which is particularly useful for modeling more complex geometries. Here, the FDTD method is used to study the effect tCTPs using a quantum-corrected model, in which a virtual conductive medium (Au Jellium) is considered in the sub-nanometer gaps of EE and FF Au NC chains. In our FDTD calculations the thickness of the substrate is infinite, while in DDA calculations, due to the constraints in the number of dipoles, a substrate of 10 nm thickness is assumed. On the other hand, in FDTD simulations, we have finite constraint on the width of the simulation region, which is set to be 1 μm in our simulations, and a perfectly matched layers (PML) region is used to approximate an infinite simulation region, but in DDA, we do not have this constraint.

Plasmonic coupling between dimers, trimers and tetramers of Au or Ag nanocubes

Using the DDA method, we have compared the near-field plasmonic coupling behavior of 21 nm Ag and AuNC dimers, trimers and tetramers with gap size of 8.5 nm in EE and FF configurations on a glass substrate (n = 1.45). Our DDA studies show that the material composition, orientation, refractive index of the cap layer, and the number of nanocubes affect the near field plasmonic coupling. As shown in Fig. 1A and B, a red shift in the extinction spectra was observed for both EE oriented Ag and Au nanocubes as the number of cubes increases.

It is found that the extent of the red shift in the plasmonic bands within the extinction spectra from dimer to tetramer in the AgNCs is comparable with the AuNCs (11.58 nm for the AgNCs and 10.38

Table 1
The intensity at maximum wavelength calculated for the extinction, absorption and scattering for Au and AgNCs in FF and EE orientations.

	FF oriented AgNCs			EE oriented AgNCs			FF oriented AuNCs			EE oriented AuNCs		
	Ext (a. u.)	Abs (a. u.)	Scat (a. u.)	Ext (a. u.)	Abs (a. u.)	Scat (a. u.)	Ext (a. u.)	Abs (a. u.)	Scat (a. u.)	Ext (a. u.)	Abs (a. u.)	Scat (a. u.)
Dimer	10.63	7.67	2.96	9.62	7.18	2.4	3.35	3.15	0.21	2.54	2.4	0.14
Trimer	15.02	8.41	6.79	10.3	6.34	3.8	5.15	4.60	0.56	3.04	2.76	0.29
Tetramer	16.51	7.89	8.58	9.15	5.18	4.01	6.51	5.57	1.00	3.14	2.87	0.38

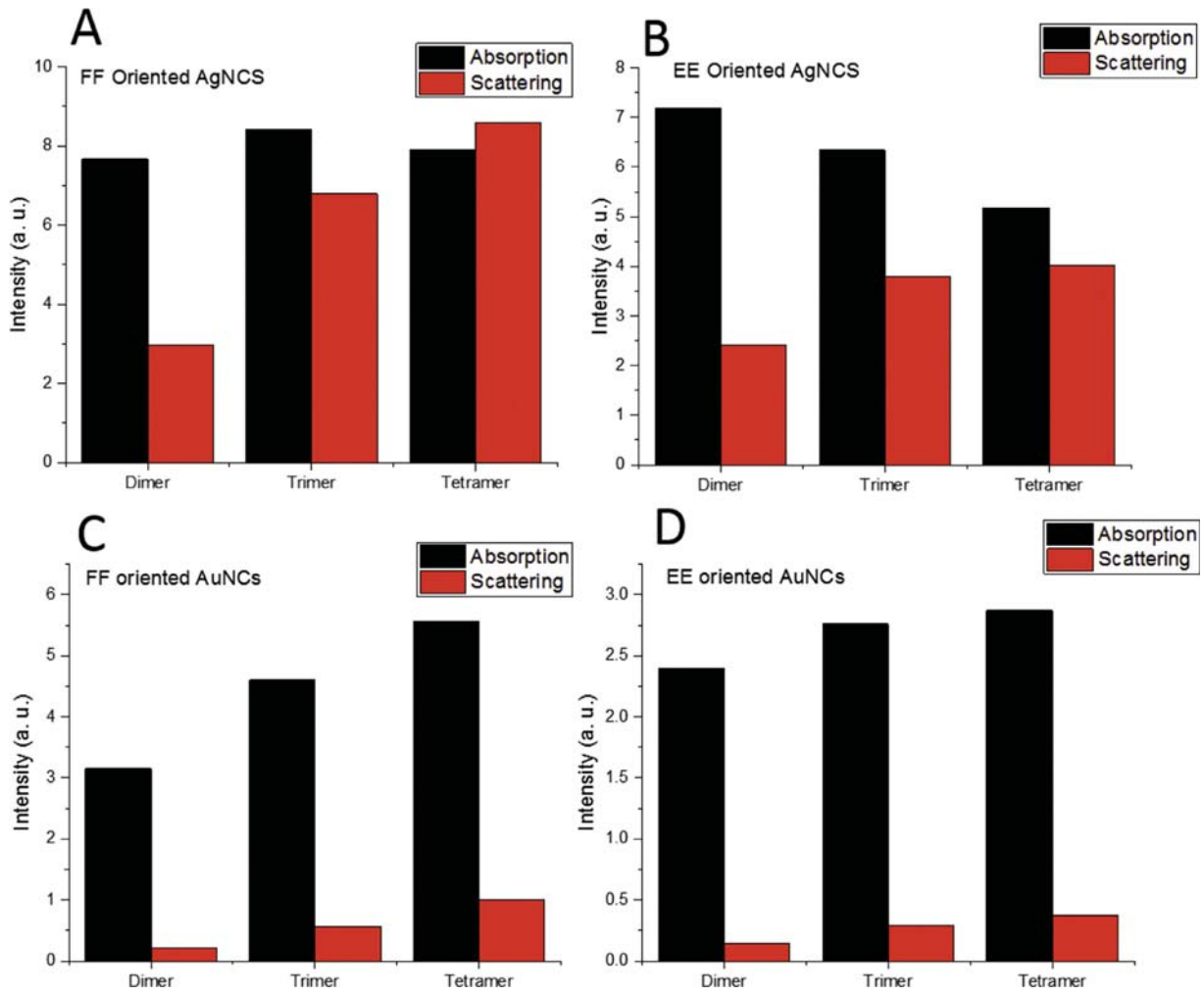

Fig. 3. The absorption and scattering cross-sections plotted as a function of the number of Ag and AuNCs in FF and EE arrangements (A–D). For the AuNCs, in both EE and FF orientations, the intensity of absorption and scattering increase as the number of cubes increases, which was absent in the FF and EE oriented AgNCs.

for the AuNCs). Interestingly, the intensity of the main LSPR band is increased as the number of the cubes is increased in AuNC chain. This monotonic increase in the extinction cross-section was not observed in the AgNC chains (Fig. 1A). Furthermore, Fig. 1B shows that the intensity of the LSPR band corresponding to quadrapole modes decreases as the number of the nanocubes increases in the Ag chains. The calculated field distribution for AgNCs shows an enhanced electromagnetic field around the adjacent edges (hot spots) and very low-intensity field region that is confined away from the adjacent edges in AgNCs. The field localization of the oscillating dipole in the region of adjacent edges of the AuNCs is weaker and more spread out around the cubes in comparison with that in the AgNCs.

The extinction spectra and the field distributions around FF-oriented Ag and AuNC chains are shown in Fig. 2. In contrast to the EE orientation of the AgNCs and AuNCs, the extinction intensity and the extent of red shift of the main LSPR band from dimer to tetramer is significantly different in AgNCs and AuNCs (~24 nm for the AgNCs and ~17 nm for the AuNCs). This could be due to the fact that the stability of the system is strongly affected due to the orientation of the cubic nanoparticles in the EE configuration [51]. One possible reason is that the repulsion between the dipoles in the FF orientation could be less than that of the EE orientation. As the dipoles spread around the large area, the main band corresponding to the dipolar modes significantly red-shifted to longer wavelengths (lower energy) in comparison with the EE arrangement.

It is found that the plasmon band corresponding to the quadrupole modes in the FF oriented AgNCs becomes nearly unchanged when the number of the cubes increases, whereas the dipolar mode is continuously red-shifted (Fig. 2B). Furthermore, the maximum field enhancement factor around the AgNCs was nearly ten times greater than that of the AuNCs under similar conditions. A typical TEM image of AuNCs[51] shows the distinct FF arrangement of the nanocubes, which further validates that the FF orientation is energetically more favorable than the EE configuration.

Table 1 shows the intensities of the extinction, absorption and scattering in two different orientations for the dimer, trimer and tetramer of the Au and the AgNCs. For the FF and EE oriented AuNCs, the extent of the absorption in comparison to scattering increases as the number of cubes increases and the extent of the absorption is much higher than the scattering in both FF and EE orientations (see Supporting Information, Figs. S1 and S2). However, AgNCs show different behavior as the orientation and the number of cubes changes. As it is shown in Fig. 3, for the EE oriented AgNCs, from dimer to tetramer, the amount of the scattering slightly changes whereas the amount of the absorption continuously decreases (see Supporting Information, Figs. S3 and S4). In contrast to the EE AgNCs, the extent of absorption for the FF AgNCs becomes nearly unchanged and the intensity of the scattering increases as the number of cubes increases (Fig. 3A and Supporting Information, Fig. S4).

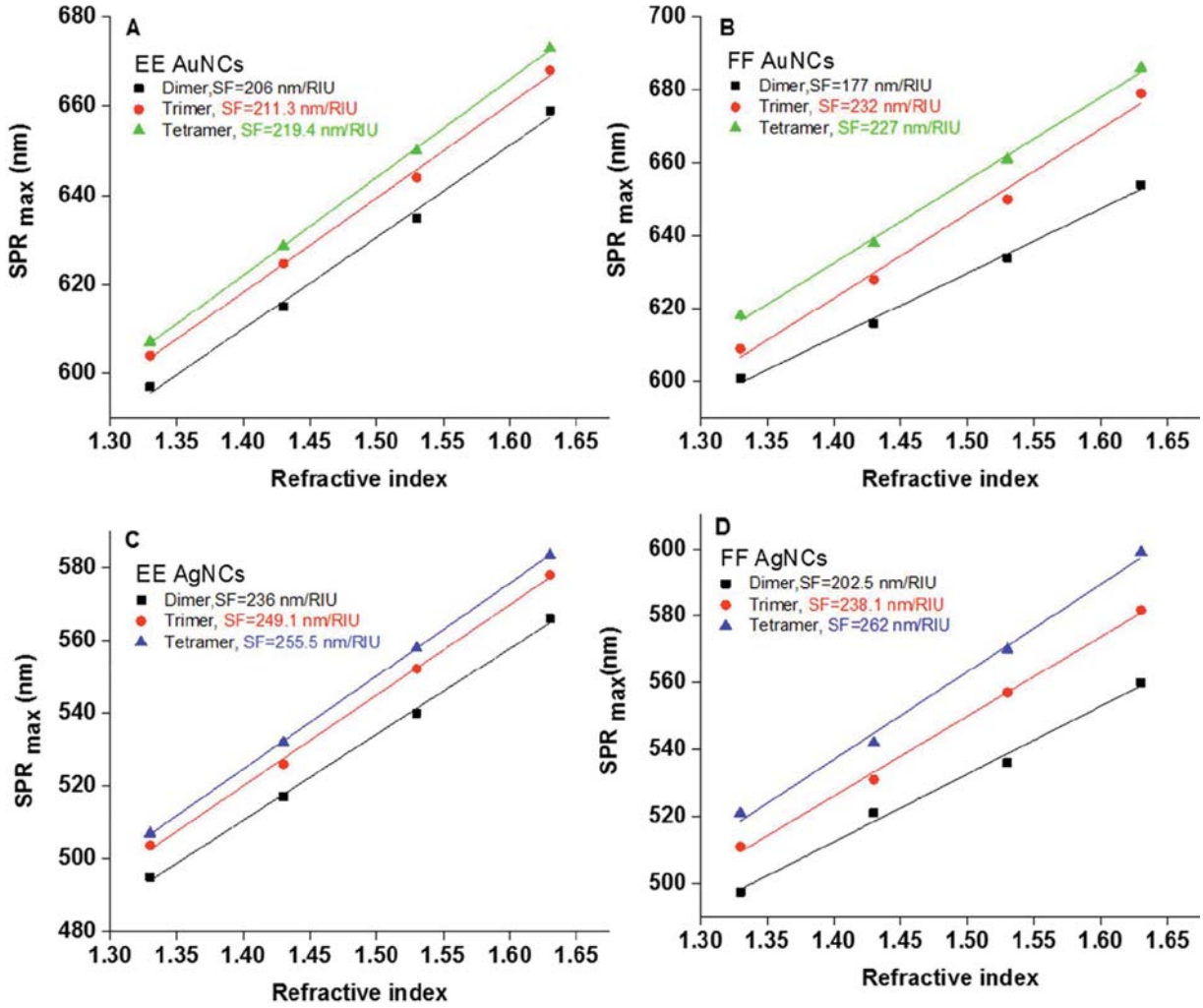

Fig. 4. Calculated SF for the FF and EE oriented Au and AgNCs (A–D). The SF was determined by liner regression of the LSPR maximum against of refractive index of medium. It shows that the SF increases as a function of the number of nanocubes.

These results imply that any variation in the metal type and mode of arrangement can result in significant variation in sensing behavior of nanoparticle-based optical sensors in imaging and sensing applications.

The magnitude of the observed shift of the main plasmonic band per unit change of the refractive index of the surrounding medium or sensitivity factor (SF) was calculated for the chains of the Au and AgNCs.

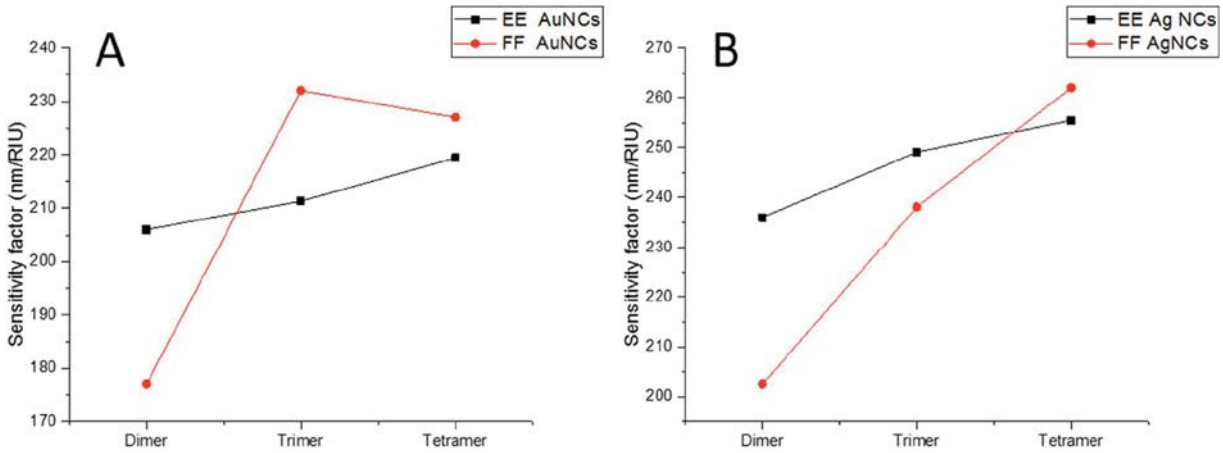

Fig. 5. Sensitivity factors for Au and Ag NCs assemblies of different orientations (EE and FF) calculated at various refractive index of surrounding medium with a 0.1 increment (from 1.33 to 1.63) and plotted as a function of the number of the cubes.

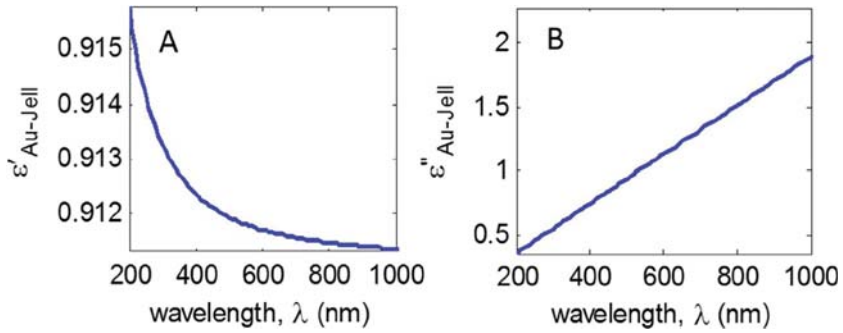

Fig. 6. (A and B) real and imaginary part of the permittivity of the Au Jellium for the case of 0.2 nm separation.

We noticed that the SF for the chains of the Au and AgNCs is highly dependent on the number of adjacent cubes. Furthermore, in comparison to FF orientation, increasing the refractive index of surrounding medium with a 0.1 increment (from 1.33 to 1.63) resulted in a noticeable increase in the average value of the SF in EE orientation in both AuNCs and AgNCs from dimer to tetramer. Interestingly, for the FF oriented Ag chains, going from the dimer to the tetramer, small changes in the SF were observed (13 nm/RIU from the dimer to the trimer and 6.4 nm/RIU from the trimer to the tetramer). However, for the EE AgNCs, we noticed a significant change in the SF, going from dimer to tetramer (36.5 nm/RIU from dimer to trimer and 24.1 nm/RIU from trimer to tetramer). Compared to the AgNCs, for the AuNCs, the magnitude of the SF was lower than AgNCs under similar conditions. We found that the SF variation from dimer to trimer is more prominent in FF AuNCs (57 nm/RIU). This shows that the sensitivity factor is dependent on the linear assembly of the plasmonic nanoparticles in terms of length and orientation, which is attributed to the reduction in the repulsion between the in-phase oscillating dipoles of a given plasmonic band, thus resulting in a red shift of its plasmonic band (Fig. 4).

Fig. 5 shows the dependence of the SF on the orientation of the Au and Ag NCs as well as the number of cubes. It is clear from both EE AuNCs and EE AgNCs that the sensitivity factor increases gradually as the number of the cubes increases. However for the FF orientation, the extent of changes in the SF is much larger than for the EE orientation under similar conditions.

Here, every individual nanocube in the nanocubes chain can be considered as an independent nanoresonator, which is strongly coupled to the adjacent resonators. The optical coupling between the plasmonic nanocubes in their resonance wavelength results in a red-shift in LSPR resonance. Furthermore, it pulls the electromagnetic field out of the metal inside the sensing region, which results in a higher electromagnetic field in the hotspots region and thus higher SF. The relative configuration of the nanocubes (FF or EE) and the separation distance determine the plasmonic coupling between the resonators and the confinement of energy in the hot spots. In addition, increasing the number of the nanocubes in a chain also increases the overall scattering and scattering cross-sections of the chain. This means that the more of the excitation beam intensity is coupled to the chain, leading to higher energy density in the hotspots and these lead to an increase in the sensitivity.

Quantum tunneling limit

So far, we have studied the response of nanocube chain at separation distances above 1 nm. In sub-nanometer separation distances, however, the electrons and thus the plasmon can tunnel through the dielectric gap and significantly alter the response of the plasmonic system [50–52]. Here, we discuss the effect of tunneling-induced charge transfer plasmons (tCTPs) on the spectral response and the electromagnetic field distribution of the nanocube chains at very short separation gaps, where the effect of quantum tunneling becomes prominent particularly in smaller nanoparticles. Since the DDA used so far in the manuscript is a purely classical method, it is beyond its capacity to describe any effect arising from the quantized nature of the plasmons or the photons, such as plasmon tunneling at sub-nanometer distances. Hence, we employed a quantum corrected model, which we chose to implement within the FDTD framework. This is a very important consideration in practical nanocube sensors as the common method of dispersing chemically synthesized nanoparticles on substrates naturally creates chains with very small gaps. Experimentally, it is also possible to control the gap between nanoparticles by coating them with chemical ligands of various lengths.

In order to study the effect of quantum tunneling on the LSPR resonance, we performed a set of simulations for a pair of small nanocubes with the edge length of 21 nm at 0.2 nm separation distance. The first simulation is a pure electromagnetic simulation using FDTD method, which does not account for the effect of plasmon tunneling. Secondly, the quantum-corrected model (QCM) was used to approximate the effect of tunneling on LSPR resonance by assuming a virtual conducting medium (Au Jellium) of 0.2 nm width between the two nanocubes. The permittivity of the tunneling channel has been calculated using the Drude model (Eq. (1)), and the tunneling damping parameters γ_g, ω_g and ε_∞ were extracted from [52].

$$\varepsilon(l,\omega) = \varepsilon_\infty - \frac{{\omega_g}^2}{\omega\left(\omega + i\gamma_g(l)\right)} \tag{1}$$

The real and imaginary part of this complex permittivity is plotted in Fig. 6. This approximation is only true if the radii of the curvature are large compared to the separation distance between the two nanocubes as well as the Fermi electron wavelength. In the case of nanocubes with sharper edges, this model can potentially break down. Previously, quantum tunneling between two relatively large nanocubes has been observed in the FF configuration [52]. As we shall see in the EE configuration, this effect is even stronger, which can be due to the higher localization of the plasmons in the sharp corners,

Fig. 7A–F shows the transmission spectra of dimer, trimer and tetramers of AuNCs in EE and FF orientation with 21 nm and edge length, 0.2 nm air gap and 5 nm radius of curvature at the corners with and without considering the effect of plasmon tunneling. As it can be inferred from these figures, the effect of tCTPs becomes significant particularly for long wavelengths, where a considerable damping of LSPR resonance peaks can be observed as a result of tunneling. The damping is also much stronger in nanocube chains with EE configuration.

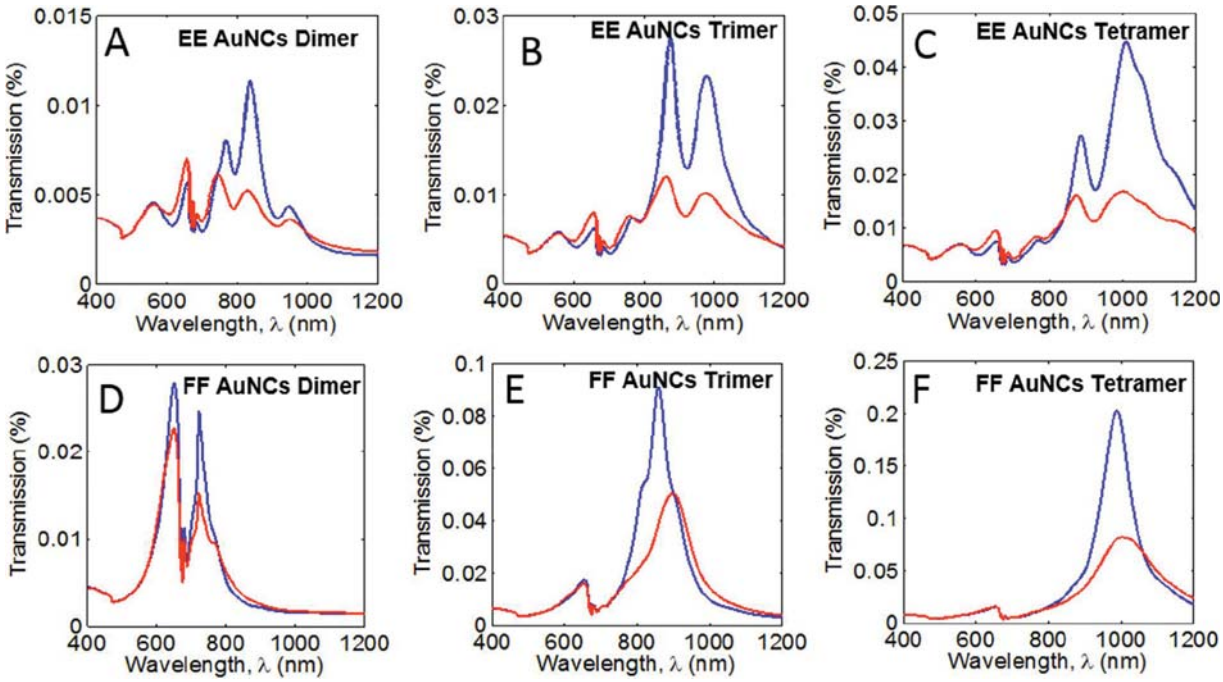

Fig. 7. (A–C) Transmission spectra for a nanocube dimer, timer and tetramer, respectively, with the 0.2 nm air gap and corner radii of 5 nm in EE and FF (D–F) configurations. Blue and red curves correspond to purely classical electromagnetic calculation and the QCM model, respectively.

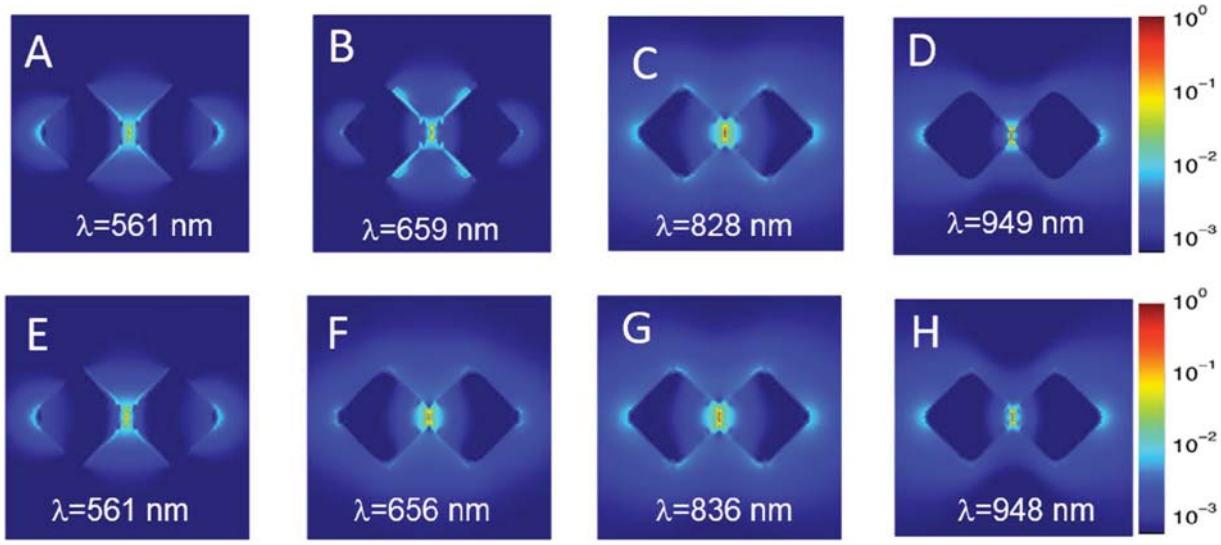

Fig. 8. Electromagnetic field distribution calculated for the EE-oriented AuNC dimer at 0.2 nm separation distance. The wavelengths of excitation were chosen based on the peak maximum for both pure electromagnetic (A–D) and quantum-corrected models (E–H).

The tunneling of charge plasmons through the metal dielectric junction at the sharp EE oriented NC chain also alters the electric field distribution profile at LSPR resonance wavelengths. Figs. 8, S5 and S6 show the electric field mode profiles of the four LSPR bands for EE AuNC dimer, trimer and tetramer at their respective λ_{res} for both pure EM and QCM models, respectively.

In general, tCTPs slightly shift the resonance wavelength and reduce the overall absorption cross-section of the plasmonic chain at resonance wavelengths as it can be seen in Fig. 6A–C for EE configuration and Fig. 6D–F for the FF configuration. In terms of the E-field distribution, as it shown in Fig. 7, the tCTPs reduce the electric-field confinement at hot-spots.

One final comment about the effect of plasmon tunneling is that even though tCTPs generally reduce the absorption (or scattering) cross-section and the intensity of electric field at the LSPR resonance wavelengths, they do not necessarily result in less sensitive sensors. The introduction of a biomolecule in the small air gap between the nanocube can change the height of the energy barrier between the two EE metal junctions and may even potentially lead to an increase in the sensitivity in the quantum-tunneling based biosensor compared to the classical sensors.

Conclusion

In conclusion, we have studied the optical properties of AuNC and AgNC chains of different lengths in FF and EE configurations using classical electromagnetic methods, at large separation gaps. Our calculations on the electric field intensity show that the EE orientation can result in greater sensitivity in LSPR-based sensing and larger enhancement factor in SERS. Secondly, the effect of tCTPs at the sharp edges of EE and FF oriented AuNC chains were studied at very small separation gaps using a quantum-corrected classical model implemented in FDTD. Our results show that the effect of plasmon tunneling in the EE-oriented NCs is even more pronounced than that of the FF-oriented NCs, due to the effect of the local topology (sharpness of the edges). Our results suggest that the EE nanocube chains can be more appealing in developing efficient sensing platforms via SERS or LSPR-based sensing in comparison with the FF chains.

Acknowledgement

The authors would like to acknowledge the Georgia Institute of Technology for providing high performance computing resources and support. The authors thank B. T. Draine and P. J. Flatau for use of their DDA Cod DDSCAT 6.1. The financial support of NSF-DMR grant (1644354) is greatly appreciated.

Appendix A. Supplementary data

Supplementary data associated with this article can be found, in the online version, at https://doi.org/10.1016/j.nantod.2017.10.009.

References

[1] S.A. Maier, IEEE J. Sel. Top. Quantum Electron. 12 (2006) 1214.
[2] K.-S. Lee, M.A. El-Sayed, J. Phys. Chem. B. 110 (2006) 19220.
[3] K.A. Willets, R.P. Van Duyne, Annu. Rev. Phys. Chem. 58 (2007) 267.
[4] J. Zhao, A. Das, G.C. Schatz, S.G. Sligar, R.P. Van Duyne, J. Phys. Chem. C 112 (2008) 13084.
[5] J.N. Anker, W.P. Hall, O. Lyandres, N.C. Shah, J. Zhao, R.P. Van Duyne, Nat. Mater. 7 (2008) 442.
[6] M.L. Brongersma, N.J. Halas, P. Nordlander, Nat. Nanotechnol. 10 (2015) 25.
[7] I.H. El-Sayed, X.H. Huang, M.A. El-Sayed, Nano Lett. 5 (2005) 829–834.
[8] H.J. Wu, J. Henzie, W.C. Lin, C. Rhodes, Z. Li, E. Sartorel, J. Thorner, P.D. Yang, J.T. Groves, Nat. Methods. 9 (2012) 1189.
[9] A.D. McFarland, R.P. Van Duyne, Nano Lett. 3 (2003) 1057.
[10] A.K. Yang, M.D. Huntington, M.F. Cardinal, S.S. Masango, R.P. Van Duyne, T.W. Odom, Acs Nano 8 (2014) 7639.
[11] S. Linic, U. Aslam, C. Boerigter, M. Morabito, Nat. Mater. 14 (2015) 567–576.
[12] S.R. Panikkanvalappil, S.M. Hira, M.A. Mahmoud, M.A. El-Sayed, J. Am. Chem. Soc. 136 (2014) 15961.
[13] S.R. Panikkanvalappil, S.M. Hira, M.A. El-Sayed, Chem. Sci. 7 (2016) 1133.
[14] E. Hao, G.C. Schatz, J. Chem. Phys. 120 (2004) 357–366.
[15] S. Link, M.A. El-Sayed, J. Phys. Chem. B 103 (1999) 8410–8426.
[16] S. Mukherjee, H. Sobhani, J.B. Lassiter, R. Bardhan, P. Nordlander, N.J. Halas, Nano Lett. 10 (2010) 2694.
[17] C.P. Byers, H. Zhang, D.F. Swearer, M. Yorulmaz, B.S. Hoener, D. Huang, et al., Sci. Adv. 1 (2015).
[18] K.L. Kelly, E. Coronado, L.L. Zhao, G.C. Schatz, J. Phys. Chem. B 107 (2002) 668.
[19] W.A. Murray, B. Auguié, W.L. Barnes, J. Phys. Chem. C 113 (2009) 5120.
[20] C.L. Haynes, R.P. Van Duyne, J. Phys. Chem. B 105 (2001) 5599.
[21] P.K. Jain, K.S. Lee, I.H. El-Sayed, M.A. El-Sayed, J. Phys. Chem. B 110 (2006) 7238.
[22] E. Ringe, J.M. McMahon, K. Sohn, C. Cobley, Y. Xia, J. Huang, et al., J. Phys. Chem. C 114 (2010) 12511.
[23] L.M. Liz-Marzán, Langmuir 22 (2005) 32.
[24] L.J. Sherry, S.-H. Chang, G.C. Schatz, R.P. Van Duyne, B.J. Wiley, Y. Xia, Nano Lett. 5 (2005) 2034.
[25] S. Link, Z.L. Wang, M.A. El-Sayed, J. Phys. Chem. B 103 (1999) 3529.
[26] H. Cha, J.H. Yoon, S. Yoon, Acs Nano. 8 (2014) 8554.
[27] C. Tabor, D. Van Haute, M.A. El-Sayed, Acs Nano. 3 (2009) 3670.
[28] A.M. Funston, C. Novo, T.J. Davis, P. Mulvaney, Nano Lett. 9 (2009) 1651.
[29] L.S. Slaughter, Y.P. Wu, B.A. Willingham, P. Nordlander, S. Link, Acs Nano. 4 (2010) 4657.
[30] N. Hooshmand, J.A. Bordley, M.A. El-Sayed, J. Phys. Chem. Lett. 5 (2014) 2229.
[31] N. Hooshmand, D. O'Neil, A.M. Asiri, M. El-Sayed, J. Phys. Chem. A 118 (2014) 8338.
[32] J.A. Bordley, N. Hooshmand, M.A. El-Sayed, Nano Lett. 15 (2015) 3391.
[33] N. Hooshmand, J.A. Bordley, M.A. El-Sayed, J. Phys. Chem. C 119 (2015) 15579.
[34] N. Hooshmand, S.R. Panikkanvalappil, M.A. El-Sayed, J. Phys. Chem. C 120 (2016) 20896.
[35] Y. Wu, P. Nordlander, J. Phys. Chem. C 114 (2010) 7302.
[36] S.H. Shams Mousavi, A.A. Eftekhar, A.H. Atabaki, A. Adibi, ACS Photonics 2 (2015) 1546.
[37] S.A. Maier, P.G. Kik, H.A. Atwater, S. Meltzer, E. Harel, B.E. Koel, A.A.G. Requicha, Nat. Mater. 2 (2003) 229.
[38] S.A. Maier, P.G. Kik, H.A. Atwater, Appl. Phys. Lett. 81 (2002) 1714.
[39] S.A. Maier, P.G. Kik, H.A. Atwater, Phys. Rev. B 67 (2003) 205402.
[40] S.S. Aćimović, M.P. Kreuzer, M.U. González, R. Quidant, ACS Nano 3 (2009) 1231.
[41] S. Enoch, R. Quidant, G. Badenes, Opt. Express 12 (2004) 3422.
[42] A. Klinkova, H. Thérien-Aubin, A. Ahmed, D. Nykypanchuk, R.M. Choueiri, B. Gagnon, et al., Nano Lett. 14 (2014) 6314.
[43] J. Becker, A. Trügler, A. Jakab, U. Hohenester, C. Sönnichsen, Plasmonics 5 (2010) 161.
[44] J.N. Anker, W.P. Hall, O. Lyandres, N.C. Shah, J. Zhao, R.P. Van Duyne, Nat. Mater. 7 (2008) 442.
[45] S.Y. Lee, L. Hung, G.S. Lang, J.E. Cornett, I.D. Mayergoyz, O. Rabin, ACS Nano 4 (2010) 5763.
[46] S. Mitiche, S. Marguet, F. Charra, L. Douillard, J. Phys. Chem. C 121 (2017) 4517.
[47] B.T. Draine, P.J. Flatau, J. Opt. Soc. Am. A 11 (1994) 1491.
[48] P.B. Johnson, R.W. Christy, Phys. Rev. B 6 (1972) 4370.
[49] W.H. Yang, G.C. Schatz, R.P. Vanduyne, J. Chem. Phys. 103 (1995) 869.
[50] T.R. Jensen, G.C. Schatz, R.P. Van Duyne, J. Phys. Chem. B 103 (1999) 2394–2401.
[51] S.R. Panikkanvalappil, M. James, S.M. Hira, J. Mobley, T. Jilling, N. Ambalavanan, M.A. El-Sayed, J. Am. Chem. Soc. 138 (2016) 3779.
[52] S.F. Tan, L. Wu, J.K.W. Yang, P. Bai, M. Bosman, C.A. Nijhuis, Science 343 (2014) 1496.

Nasrin Hooshmand is a Research Scientist at the Georgia Institute of Technology. She received her MSc from Shiraz University (Iran), and received her Ph.D. degree from Tehran SRBIAU (Iran) in the field of Physical Chemistry. Her research interests are focused on understanding the unique features of the most sensitive assembled nanostructures made of gold and/or silver plasmonic nanoparticles. She has developed and contributed to important discoveries in nanoplasmonics and spectroscopy and their potential use in the fields of sensing and bio-sensing. She is applying the important theoretical results obtained from the plasmonic properties of different assemblies and morphologies of gold nanoparticles for their utilization in the diagnosis and photo-thermal treatment of cancer. Special interest is focused on carrying out nanoscience and nanotechnology as the computational methods to find new material with new properties in Plasmonic Nanotechnology.

S. Hamed Shams Mousavi received his B.Sc. in electrical engineering from University of Tehran, Iran and his M.Sc. from Ecole Superieure d'Electricite (Supelec), France. He joined the Photonics Research Group at Georgia Institute of Technology in Spring 2011 where he is now a Ph.D. student. His current research interests lie in plasmonics, integrated photonics and light-matter interaction.

Sajanlal Panikkanvalappil received his Ph.D. degree in Physical Chemistry from Indian Institute of Technology Madras in 2011. Currently, he is working as a postdoctoral research fellow in the School of Chemistry and Biochemistry at Georgia Institute of Technology, Atlanta, USA. His research focuses on exploring novel routes to synthesize technically relevant nanomaterials, formulating ultrasensitive sensors and developing nanotechnology-based techniques to understand biomolecular events in cancer cells as well as to diagnose and selectively destruct them at its early stages using plamonic nanoparticles-based techniques. He has authored or co-authored more than 35 well-cited scientific articles, two book chapters, two patents and ten patent applications, in the most prestigious journals in the fields of material science and nanotechnology. He has received several awards for his research excellence including 'Langmuir Prize' for the best Ph.D. thesis in Physical and Theoretical Chemistry by Indian Institute of Technology Madras and "Young Researcher Award" at the Chennai Chemistry Conference in 2011.

Ali Adibi is the director for the Center for Bio and Environmental Sensing Technologies (BEST) at the Georgia Institute of Technology. He received his B.S.E.E. from Shiraz University (Iran) in 1990, and received his M.S.E.E. and Ph.D. degrees from the Georgia Institute of Technology (1994) and the California Institute of Technology (2000), respectively. His Ph.D. research resulted in a breakthrough in persistent holographic storage in photorefractive crystals. In 2000, he joined the faculty of the School of Electrical and Computer Engineering at the Georgia Institute of Technology, where he is now an associate professor. Dr. Adibi has a wide range of research interests in both theoretical and experimental aspects of photonic devices and materials.

Mostafa A. El - Sayed B.Sc., Ain Shams U. Cairo, Egypt; Ph.D., Florida State University; Postdoctoral Fellow at Yale University, Harvard University and the California Institute of Technology; Faculty member at UCLA Department of Chemistry and Biochemistry (1961-94); Julius Brown Chair and Regents' Professor, Georgia Institute of Technology Department of Chemistry and Biochemistry (1994-present) Professor El-Sayed received the 2007 US National Medal of Science in Chemistry from the President of the United States (2008) and the Medal of the Egyptian Republic of the First Class from the President of Egypt (2009). He received the US National Medal of Science in 2014, and in 2016 the American Chemical Society highest honor, the Priestley Medal.Professor El-Sayed is an Elected Member of the US National Academy of Sciences (1980), an Elected Fellow of the American Academy of Arts and Sciences (1986), an Elected Associate Member of the Third World Academy of Sciences (1984). He received the King Faisal International Prize in the Sciences (Chemistry).